Journal of
Plankton Research

plankt.oxfordjournals.org

J. Plankton Res. (2014) 36(5): 1310–1322. First published online June 12, 2014 doi:10.1093/plankt/fbu051

Ambient fluid motions influence swimming and feeding by the ctenophore *Mnemiopsis leidyi*

KELLY R. SUTHERLAND[1]*, JACK H. COSTELLO[2,3], SEAN P. COLIN[3,4] AND JOHN O. DABIRI[5]

[1]OREGON INSTITUTE OF MARINE BIOLOGY, UNIVERSITY OF OREGON, EUGENE, OR, USA, [2]BIOLOGY DEPARTMENT, PROVIDENCE COLLEGE, PROVIDENCE, RI, USA, [3]WHITMAN CENTER, MARINE BIOLOGICAL LABORATORY, WOODS HOLE, MA, USA, [4]MARINE BIOLOGY/ENVIRONMENTAL SCIENCES, ROGER WILLIAMS UNIVERSITY, BRISTOL, RI, USA AND [5]GRADUATE AERONAUTICAL LABORATORIES AND BIOENGINEERING, CALIFORNIA INSTITUTE OF TECHNOLOGY, PASADENA, CA, USA

*CORRESPONDING AUTHOR: ksuth@uoregon.edu

Received January 3, 2014; accepted May 15, 2014

Corresponding editor: Roger Harris

Planktonic organisms are exposed to turbulent water motion that affects the fundamental activities of swimming and feeding. The goal of this study was to measure the influence of realistic turbulence levels on (i) swimming behavior and (ii) fluid interactions during feeding by the lobate ctenophore, *Mnemiopsis leidyi*, a highly successful suspension-feeding predator. A laboratory turbulence generator produced turbulence ($\varepsilon = 0.5–1.4 \times 10^{-6}$ W kg^{-1}) representative of a field site in Woods Hole, MA, USA. Compared with still water, *M. leidyi* avoided regions in the experimental vessel where turbulence was greatest ($\varepsilon = 1.1–1.4 \times 10^{-6}$ W kg^{-1}) by increasing its swimming speeds and accelerations. Both laboratory and *in situ* particle image velocimetry data demonstrated that feeding currents of *M. leidyi* were eroded by ambient fluid motions. Despite this, the overall flux to the feeding structures remained constant due to higher swimming speeds in turbulent conditions. Instantaneous shear deformation rates produced by background turbulence were higher than those produced by ctenophore feeding currents and frequently exceeded the published escape thresholds of copepod prey. Feeding current erosion and fluid mechanical signal noise within turbulent flows affect the mechanics of predator–prey interactions during suspension feeding by the ctenophore *M. leidyi*.

KEYWORDS: *Mnemiopsis leidyi*; turbulence; swimming behavior; suspension feeding

INTRODUCTION

Interactions between planktonic predators and prey in the ocean occur within moving fluids. In coastal systems, turbulent fluid motion, stochastic flow at the organism-scale, is particularly ubiquitous and prevalent. Physical structures generated by turbulence interact with plankton

Downloaded from http://plankt.oxfordjournals.org/ at Acquisitions Dept-Serials on September 9, 2014

© The Author 2014. Published by Oxford University Press. All rights reserved. For permissions, please email: journals.permissions@oup.com

at the organism-scale to influence basic processes, including encounter, escape behaviors and ingestion (see Fig. 2 in Prairie *et al.*, 2012), ultimately shaping trophic interactions, distributions and abundances. Theoretical and laboratory studies show that turbulence affects encounters with prey by ambush predators (Rothschild and Osborn, 1988; Peters and Gross, 1994; Saiz and Kiørboe, 1995). However, the majority of bloom-forming gelatinous predators can be characterized as suspension feeders and the effect of turbulence on this feeding mode is less understood. Ingestion rates of ambush predators peak at intermediate levels of turbulence due to increasing contact rates and decreasing capture probabilities with increases in turbulence level (Pésceli *et al.*, 2012). In suspension-feeding organisms, however, intermediate levels of turbulence may degrade the feeding current, resulting in lower encounter rates (Marrasé *et al.*, 1990; Saiz and Kiørboe, 1995). Studies of suspension feeders are limited and direct, *in situ* measurements have remained intractable. Furthermore, this foraging strategy, coupled with low body carbon associated with being gelatinous, is highly energetically efficient (Acuña, 2001; Pitt *et al.*, 2013), thereby placing ctenophores and other gelatinous zooplankton in a unique position to proliferate under changing ocean conditions (Mills, 1995; Costello *et al.*, 2012).

The lobate ctenophore, *Mnemiopsis leidyi* (recognized as a monospecific genus; Costello *et al.*, 2012), is an example of a gelatinous predator that has gained substantial attention due to its success as a key predator in both its endemic habitat, along the Atlantic coast of north and south America, and in introduced habitats throughout Europe (for reviews, see Purcell *et al.*, 2001; Costello *et al.*, 2012). In spite of its capacity to reduce zooplankton standing stock and diversity (e.g. Finenko *et al.*, 2006; Kideys *et al.*, 2008; Roohi *et al.*, 2009), we lack a basic understanding of how behavior and feeding are influenced under natural, environmental fluid conditions.

During feeding, *M. leidyi* generates a steady, laminar feeding current between the lobes by beating cilia lining the auricles (Fig. 1). This mode of feeding is not only effective for processing large fluid volumes but also generates a minimal fluid signature outside the lobes (Colin *et al.*, 2010). Slow-swimming and non-motile prey are entrained into the feeding current, and transported to the tentillae (oral tentacles) (Waggett and Costello, 1999). Motile prey, primarily copepods, are not generally entrained by the feeding current and instead typically swim into contact with oral lobe surfaces. Owing to the minimal fluid signature generated by the slow, laminar feeding current, motile prey capable of responding to hydromechanical signals are unlikely to detect a fluid signal until they are already positioned between the lobes where shear deformation levels are elevated (Colin *et al.*, 2010). At this point, if the prey detects the elevated shear and elicits an escape response, the ctenophore responds to the hydromechanical disturbance induced by the copepod by altering its lobe position, which minimizes available openings for escape. As a result, copepods that trigger an anticipatory response by the ctenophore, i.e. an alteration in lobe position, are more likely to be captured (Costello *et al.*, 1999). The predation process is thus a complex interplay between behaviors of the predator and prey as well as the associated fluid mechanics. These interactions are further complicated by environmental turbulence.

In addition to structuring fluid interactions during feeding, there is evidence that turbulence is important in regulating behavior and vertical distributions of *M. leidyi* in the field. Previous work documents avoidance of windy or highly mixed surface waters by lobate ctenophores, particularly *M. leidyi* (Miller, 1974; Mutlu, 1999;

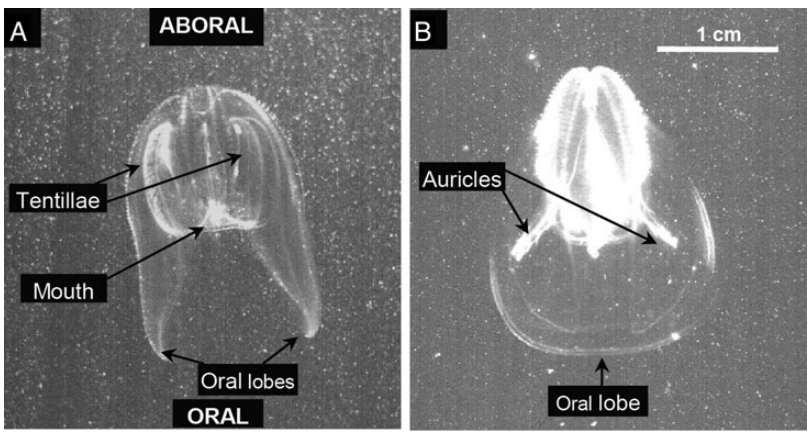

Fig. 1. Side view (**A**) and lobe view (**B**) PIV images of *M. leidyi* showing basic morphological features involved in feeding.

Downloaded from http://plankt.oxfordjournals.org/ at Acquisitions Dept-Serials on September 9, 2014

Purcell *et al.*, 2001; Costello and Mianzan, 2003). In waters characterized by a pronounced thermocline, *M. leidyi* may migrate into or below the thermocline during periods of high surface mixing (Mianzan *et al.*, 2010). However, the behavioral mechanisms that account for these changes in vertical distribution have not been quantified.

The overarching goal of this work was to understand how turbulence mediates trophic interactions by an important filter feeder. In the present study, we examined how realistic levels of turbulence influence: (i) swimming trajectories and behaviors in a laboratory turbulence generator and (ii) fluid interactions during feeding *in situ* and in a laboratory turbulence generator.

METHOD

All ctenophore collections and field measurements were made from docks near the Marine Biological Laboratory, Woods Hole, MA, USA (41°31′28.992″, −70°40′22.6842″) during July and August in 2010, 2011 and 2012. Experimental animals were collected by hand, maintained at ambient field temperature (21–23°C) and used within 8 h of collection.

Turbulence generation in the laboratory

The effect of turbulence on swimming behavior and fluid interactions during feeding was investigated using a 38 L (dimensions = 50 × 26 × 30 cm, width × depth × height) laboratory turbulence generator designed to approximate realistic environmental turbulence. Following the design of Warnaars *et al.* (2006), momentum was imparted to the fluid using two underwater speakers (diameter = 21 cm; Clark Synthesis AQ339) mounted in the center of each side wall on opposite sides of the tank. Sine waves (frequency = 30 Hz, phase = 180°) were generated using Test Tone Generator (Timo Esser) and delivered to an amplifier (Samson Servo 200), which was connected to the speakers. Stainless steel grids with 1 cm^2 openings (mesh diameter = 0.25 cm) mounted in front of the speakers generated small-scale fluid structures (grid separation distance = 32 cm).

Measurement of laboratory turbulence for swimming behavior experiments

To determine the influence of turbulence on swimming behavior, ctenophores were exposed to two treatments in the turbulence generator: still water and turbulence [$\varepsilon \sim 10^{-7}$ W kg^{-1}; a turbulence kinetic energy (TKE) dissipation rate representative of a moderate level of turbulence in the field]. Prior to behavioral measurements, TKE dissipation rate was determined through separate particle image velocimetry (PIV) measurements. Neutrally buoyant, 10 μm glass beads were seeded into the tank and illuminated using a 300 mW continuous green laser (532-nm wavelength). The motion of the particles was imaged using a Sony HDR-HC9 camcorder (1440 × 1080 pixels) at 30 frames s^{-1}. For the present study, u and w are the two velocity components in orthogonal directions x and z. Image pairs were processed using a cross-correlation PIV algorithm with an interrogation window size of 32 × 32 pixels and a 50% overlap to produce u and w velocity vectors and vorticity ($\omega_y = \partial w/\partial x - \partial u/\partial z$) maps (LaVision software). For estimates of the overall turbulence level, the 8.5 × 13.8 cm field-of-view was in the center of the tank. For vertical estimates of turbulence, the field-of-view was centered in the tank between the front and back walls and three measurements were made at the top, center and bottom of the tank. In each case, 100 pairs of frames were analyzed. To put tank turbulence levels in the context of field levels, we examined wind data from a local weather station located at the Woods Hole Oceanographic Institution (within 150 m of the sampling location) and made vertical velocity measurements from the surface to the bottom at ~30 cm intervals from a dock using an Acoustic Doppler Velocimeter (ADV; Nortek vector).

Calculation of turbulence kinetic energy

The mean TKE dissipation rate, ε, from laboratory and field measurements, was computed directly from the 2D velocity vector maps (de Jong *et al.*, 2009).

$$\varepsilon = 4\nu\left[\left\langle\left(\frac{\partial u}{\partial x}\right)^2\right\rangle + \left\langle\left(\frac{\partial w}{\partial z}\right)^2\right\rangle + \left\langle\frac{\partial u}{\partial x}\frac{\partial w}{\partial z}\right\rangle + \frac{3}{4}\left\langle\left(\frac{\partial u}{\partial x}\frac{\partial w}{\partial z}\right)^2\right\rangle\right], \quad (1)$$

where ν is the kinematic viscosity of the seawater. Estimation of dissipation rate from the 2D data assumes that turbulence is isotropic and homogeneous. Although these criteria were not fully met in the experimental system, the ratio of u_{rms} to w_{rms} did not deviate substantially from 1 (range: 0.62–0.95) and the dissipation rates at different depths in the turbulence generator were within one order of magnitude (Table I). Random measurement error (e.g. from noise in the PIV data) was addressed using the correction of Tanaka and Eaton (2007), which isolates noise in the PIV measurements by

Downloaded from http://plankt.oxfordjournals.org/ at Acquisitions Dept-Serials on September 9, 2014

Table I: Characterization of flow parameters in the turbulence tank from PIV data

Depth range (cm)	$\varepsilon \times 10^{-7}$ (W kg^{-1})	η (cm)	Re_λ	u_{rms} (cm s^{-1})	w_{rms} (cm s^{-1})	$u_{\mathrm{rms}}/w_{\mathrm{rms}}$
0–3	14.0	0.12	14	0.23	0.37	0.62
3–6	11.7	0.13	14	0.22	0.35	0.63
0–10	10.3	0.13	19	0.25	0.34	0.74
10–20	8.2	0.14	28	0.28	0.30	0.95
20–30	5.2	0.16	23	0.23	0.28	0.82

comparing dissipation rate estimates for multiple interrogation window sizes.

The Kolmogorov length scale (η) the size of the smallest fluid structures, was calculated as

$$\eta = \left(\frac{\nu^3}{\varepsilon}\right)^{0.25}. \quad (2)$$

The Taylor Reynolds number (Re_λ) was calculated as

$$\mathrm{Re}_\lambda = \frac{u_{\mathrm{rms}}\,\lambda}{\nu}, \quad (3)$$

where u_{rms} is the root-mean square (rms) velocity and λ is the Taylor microscale ($\lambda = \sqrt{15\nu u_{\mathrm{rms}}^2/\varepsilon}$). The Re measures the relative importance of inertial and viscous forces; at $\mathrm{Re} \gg 1$, inertial forces dominate.

Swimming behavior

For each swimming behavior trial, four to six ctenophores [total length 3.9 ± 0.9 cm, mean $\pm$ standard deviation (SD)] were placed in the tank, allowed to acclimate for 10–12 min and filmed for 30 min with a Sony HDR-HC9 camcorder (30 frames s^{-1}). Experiments were conducted as paired trials such that the same individuals were exposed to each treatment. A total of 20 *M. leidyi* were observed in four paired trials; 10 of the 20 individuals experienced turbulence followed by still water and 10 of the 20 individuals experienced still water followed by turbulence.

The horizontal (x) and vertical (z) positions of the aboral apex of each ctenophore were digitized at 1 s intervals using ImageJ (National Institutes of Health, USA) to produce swimming trajectories relative to a fixed frame of reference. Measured swimming parameters based on the means from the four to six individuals per tank included observed speed, acceleration, mean depth and net-to-gross displacement ratio (NGDR). The NGDR is the shortest distance between the start and end points of a trajectory divided by the total distance traveled (Dicke and Burrough, 1988) and is a measure of the straightness of the trajectories. Each parameter was compared between treatments using paired t-tests after testing for normality (SigmaStat 3.5). For data visualization purposes, instantaneous measurements of depth and observed swimming speeds from the 20 individuals were also plotted in frequency distribution histograms.

Influence of turbulence on feeding currents

The volume of fluid passing to the feeding structures is directly influenced by the position of the lobes (Colin *et al.*, 2010). Distances between lobe tips and oral–aboral lengths were measured in still water and turbulence from the behavior videos described above. Lobe measurements were made using ImageJ from frames where *M. leidyi* were oriented with the side view perpendicular to the camera (Fig. 1A). Lobe width comparisons were made between ctenophores swimming in still water ($n = 13$) and turbulence ($n = 14$) using an analysis of covariance (ANCOVA) with length as the covariate after testing for homogeneity of slopes using an ANOVA (MATLAB Statistics Toolbox).

Simultaneous measurements of the feeding current and the background fluid motion in still water and turbulence were imaged in a separate set of experiments using a second PIV set-up mounted on a 3D translation system. For these measurements, a 1 W continuous red laser (671 nm wavelength) was used to illuminate 10 μm glass beads seeded into the tank and the motion of the particles was imaged using a high-speed digital video camera (Phototron Fastcam 1024 PCI, 1024×1024 pixels) at 100 frames s^{-1}. Individual feeding current sequences were recorded by tracking ctenophores with the translation system. To estimate the turbulence level local to the ctenophore, 30–120 pairs of frames were analyzed just before or just after the feeding current sequence and the field-of-view was 6.6×6.6 mm. The increment between frames that were analyzed was adjusted to ensure that particle displacements were approximately one-fourth of the interrogation window size or less. For comparison with laboratory measurements, *in situ* behavioral and fluid motion measurements were collected by divers using a self-contained underwater velocimetry apparatus (SCUVA) (Katija and Dabiri, 2008). Dives were made in close proximity to the ctenophore collection site and the maximum dive depth was ~5 m. Before analyzing the video, sequences were rotated such that the flow into the lobes was traveling directly along the z-axis. The flux of fluid passing between the lobes, which represents a theoretical maximum clearance rate, F_{max}, was calculated in still water ($n = 12$) and turbulence ($n = 14$; Colin *et al.*, 2010). F_{max} was based on the relative velocities of the ctenophore and the fluid over

Downloaded from http://plankt.oxfordjournals.org/ at Acquisitions Dept-Serials on September 9, 2014

~100 frames as follows:

$$F_{max} = Aw, \quad (4)$$

where w is the velocity vectors passing through the elliptical area (A) defined by the lobe width and interlobe gap distance (Colin *et al.*, 2010). Comparisons of F_{max} in still water and turbulence were made using an ANCOVA with length as the covariate after testing for homogeneity of slopes using an ANOVA (MATLAB Statistics Toolbox).

Some prey items, particularly copepods (Kiørboe *et al.*, 1999; Burdick *et al.*, 2007), exhibit escape behaviors in response to shear deformation. Therefore, the maximum components of the 2D shear deformation rate generated by the feeding current when ctenophores were oriented with the y-axis in the oral–aboral direction, S_{zz} and S_{zx} (Colin *et al.*, 2010), were calculated (LaVision software) for one still water case and one turbulence case:

$$S_{zz} = \frac{dw}{dz} \quad (5)$$

and

$$S_{zx} = \frac{du}{dz}. \quad (6)$$

RESULTS

Turbulence generation in the laboratory and comparison with field measurements

Representative plots of instantaneous velocity and vorticity measured with PIV in the center of the laboratory turbulence generator and in the field show that flow fields were qualitatively comparable (Fig. 2). Quantitatively, measurements were similar in terms of velocity magnitude, turbulent dissipation rate, Kolmogorov length scale and Taylor microscale Reynolds number (Fig. 2). The maximum TKE dissipation rate measured in the tank was $\sim 10^{-6}$ W kg^{-1}, which was within the range of mixed layer turbulence: 10^{-9} to 10^{-5} W kg^{-1} (Peters and Redondo, 1997; Jumars *et al.*, 2009). Taylor microscale Reynolds numbers were relatively low, consistent with field measurements at similar dissipation rates (Luznik *et al.*, 2007).

Turbulence was not homogeneous throughout the tank and instead, was highest in the top 10 cm and decreased with depth (Table I). Within the top 3 cm, the TKE dissipation rate was highest. The Kolmogorov scale and Reynolds numbers also varied slightly with depth but were within the same order of magnitude. Velocities remained consistent with depth though horizontal velocities (u) were lower than vertical velocities (w) suggesting anisotropy. The presence of anisotropy is consistent with turbulence measurements in the shallow coastal ocean (Fig. 2B), particularly when $Re_\lambda < 100$ (Luznik *et al.*, 2007).

Though the spatial scales are different, the presence of a vertical turbulence gradient in the laboratory was consistent with the vertical pattern measured in the field (Fig. 3). Turbulence calculated from vertical ADV profiles during a less windy (Fig. 3A) and more windy (Fig. 3B) time period on 14 August 2012 showed that when wind speeds were ~4-fold higher (Fig. 3C), TKE dissipation rate was higher at the surface and was also higher at each depth compared with the less windy case. In both cases, turbulence was higher at the surface and declined with depth such that the lowest turbulence levels were near the bottom. This vertical gradient approximated wind-driven turbulence and provided a refuge at depth. The ADV profiles taken during a less windy (Mean speed = 1.3 m s^{-1})

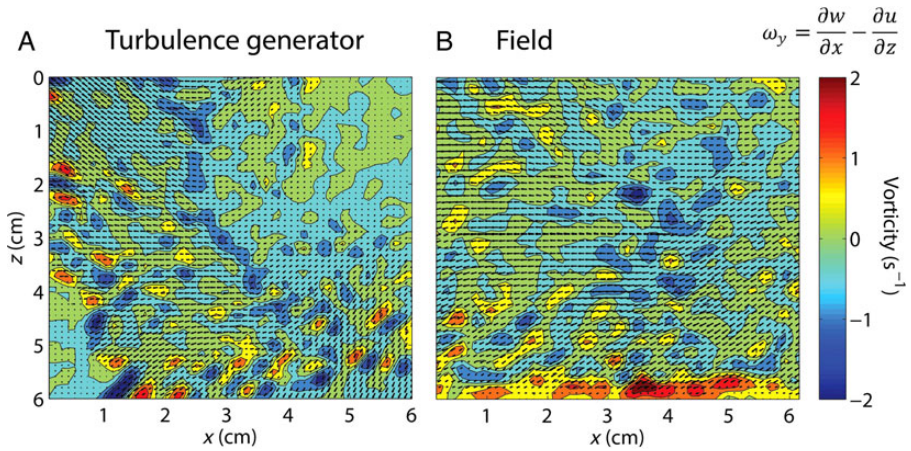

Fig. 2. Instantaneous velocity vectors (black) and vorticity contours from (**A**) the center of the turbulence generator (u_{rms} = 2.7 mm s^{-1}, w_{rms} = 2.0 mm s^{-1}, $\varepsilon = 7.1 \times 10^{-7}$ W kg^{-1}, η = 1.5 mm and Re_λ = 27) and (**B**) field measurements taken in Woods Hole, MA on 3 August 2010 (u_{rms} = 4.7 mm s^{-1}, w_{rms} = 3.9 mm s^{-1}, $\varepsilon = 7.4 \times 10^{-7}$ W kg^{-1}, η = 1.5 mm and Re_λ = 82).

Downloaded from http://plankt.oxfordjournals.org/ at Acquisitions Dept-Serials on September 9, 2014

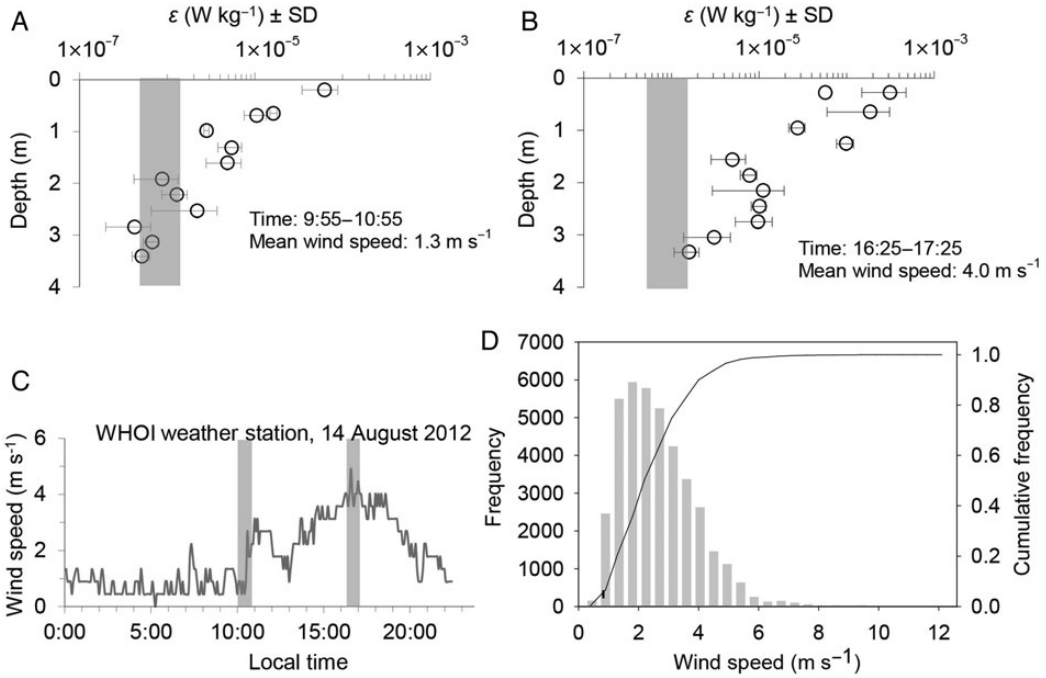

Fig. 3. Field TKE dissipation rate and winds speeds in Woods Hole, MA. Vertical profiles of field dissipation rates, ε, calculated from ADV measurements taken on 14 August 2012 at (**A**) 9:55 and (**B**) 16:25. Grey shaded areas correspond to turbulence range in laboratory experiments. Wind speeds at a local weather station are shown in (**C**) with grey shaded bars indicating approximate times when ADV measurements were taken in (A) and (B). Wind speed frequency and cumulative frequency over a single year (2012) from the weather station are shown in (**D**). Dashed lines in (D) correspond to 5, 50 and 95% of the cumulative frequency.

and more windy time period (Mean speed = 4.0 m s^{-1}; Fig. 3A and B) were representative of the lower and upper end of wind speeds over the year: the 5, 50 and 95% cumulative frequencies from wind speeds measured during 2012 were at 0.8, 2.2 and 4.7 m s^{-1}, respectively (Fig. 3D).

Swimming behavior in laboratory turbulence

In both still water and turbulence, ctenophores spent the majority of the time near the top portion of the tank and occasionally made forays deeper in the tank (Fig. 4A and C). The mean observed speed and acceleration were higher in the turbulence treatment (Table II). In still water, *M. leidyi* spent ∼45% of the time stationary (i.e. speed <0.15 cm s^{-1}), whereas in turbulence, *M. leidyi* spent only ∼32% of the time stationary (Fig. 5). The NGDR, or tortuosity of the swimming tracks, was not different between treatments (Table II). Mean depth was not significantly different between still water and turbulent treatments (Table II). However, frequency distribution plots based on instantaneous *z*-positions show a clear avoidance of the top 6 cm in turbulence (Fig. 4B and D). Higher *M. leidyi* speeds and accelerations were also measured in the top 3 cm in turbulence (Table III).

Influence of turbulence on feeding currents

Once turbulence was initiated, ctenophores were observed to briefly fold the lobes inward but lobes returned to a relaxed position within ∼10 s. Over the 30 min trial, there was no difference in lobe width in turbulent versus non-turbulent conditions (Fig. 6).

Laminar flows produced by the feeding current of *M. leidyi* in still water were characterized by flow oriented toward the oral structures. In contrast, feeding current structure was degraded in both laboratory and field turbulence (Fig. 7). Although feeding current structure was degraded in turbulent flows, the overall flux of fluid between the lobes, F_{max}, was not significantly different in still water and turbulence (Fig. 8) due to higher swimming speeds in turbulence (Table II). In addition, instantaneous shear deformation rates produced by background turbulence in the laboratory and field were frequently higher than those within the feeding current (Fig. 9). In still water, instantaneous deformation rates that are high enough to produce escape responses by common coastal copepod species only occurred well within the lobes as a result of the feeding current (Fig. 9A and D). In turbulence, on the other hand, instantaneous deformation rates that are high enough to elicit escapes occurred outside of the lobes as well as within the lobes due to the

Downloaded from http://plankt.oxfordjournals.org/ at Acquisitions Dept-Serials on September 9, 2014

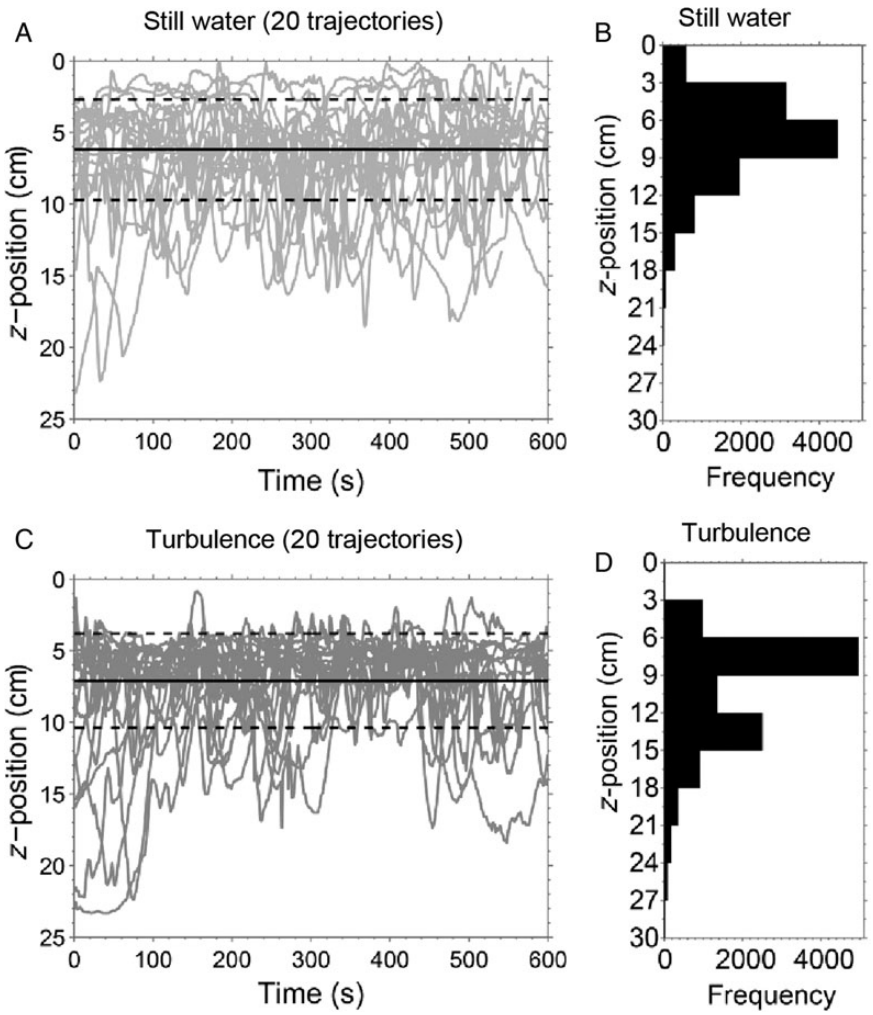

Fig. 4. Swimming depth (z) with time measured from 20 individuals in each treatment (**A** and **C**) and depth distribution frequency histograms of *M. leidyi* from all instantaneous z-positions (**B** and **D**) measured in still water (11 422 observations) and turbulence (11 346 observations, $\varepsilon \sim 10^{-7}\,\mathrm{W\,kg^{-1}}$).

Table II: Mnemiopsis leidyi swimming behavior in the turbulence tank (mean ± SD)

Flow condition	Observed speed (cm s^{-1})	Acceleration (cm s^{-2})	NGDR	Depth (cm)	n
Still water	0.27 ± 0.08	0.14 ± 0.04	0.40 ± 0.14	6.2 ± 0.3	4
Turbulence	0.33 ± 0.09	0.18 ± 0.05	0.43 ± 0.14	7.4 ± 1.0	4
	$t = 3.80$	$t = 3.64$	$t = 1.51$	$t = 2.64$	
	df = 3	df = 3	df = 3	df = 3	
	$P = 0.032$	$P = 0.036$	$P = 0.23$	$P = 0.08$	

T-test statistics and *P*-values for paired comparisons between still water and turbulence are presented at the bottom of each column. n is the number of individual tanks (four to six ctenophores per tank) observed in each treatment.

influence of background turbulence (Fig. 9C and F). Frequency histograms of the instantaneous shear deformation rate (S_{zx}) for the individuals shown in Fig. 9A and C measured over 10 frames, corresponding to 1.67 s in still water and 0.33 s in turbulence, show that deformation rates were more variable in turbulence and frequently exceeded the escape threshold of copepod prey (Fig. 10).

DISCUSSION

In the natural environment, planktonic organisms are exposed to a range of water motions that mediate fundamental activities, including swimming and feeding. The results from this study show that *M. leidyi* have a behavioral response of increased swimming activity to even moderately low levels of turbulence that are common in coastal regions in the mid-water column. Furthermore, moderate levels of turbulence can potentially influence *M. leidyi* feeding by degrading fluid structures generated by the feeding current (though flux is not affected) and

Downloaded from http://plankt.oxfordjournals.org/ at Acquisitions Dept-Serials on September 9, 2014

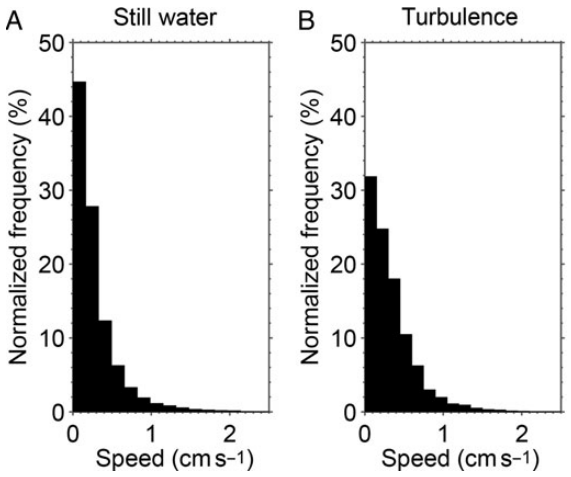

Fig. 5. Frequency histograms showing observed speed of *M. leidyi* from all instantaneous velocity measurements (11 422 observations) from 20 individuals in still water (**A**) and turbulence (11 346 observations, $\varepsilon \sim 10^{-7}$ W kg^{-1}) (**B**). Relative numbers of speed observations are expressed as percentages.

Table III: Swimming speed and acceleration of M. leidyi within the top 6 cm and top 3 cm of the tank calculated from instantaneous measurements from 20 individuals in still water and 20 individuals in turbulence ($\varepsilon \sim 10^{-7}$ W kg^{-1}) conditions

Flow condition	Depth range (cm)	Observed speed (cm s^{-1})	Acceleration (cm s^{-2})	Number of instantaneous observations
Still water	0–6	0.24	0.16	6261
Still water	0–3	0.21	0.15	1795
Turbulence	0–6	0.27	0.17	4438
Turbulence	0–3	0.96	0.93	61

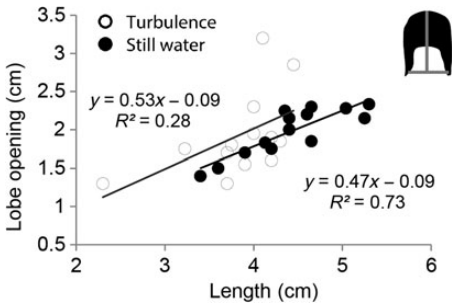

Fig. 6. Lobe position, measured as distance between lobe tips, versus total ctenophore length measured in the turbulence tank in still water and turbulence ($\varepsilon \sim 10^{-7}$ W kg^{-1}). The inset to the right indicates how length and lobe opening were measured. There was no difference in lobe width in turbulent versus non-turbulent conditions (ANCOVA, $F_{1,23} = 0.05$, $P = 0.83$).

obscuring fluid mechanical signals that cue predatory responses by the ctenophore as well as escape responses by motile prey.

Swimming behavior in laboratory turbulence

Under both still and turbulent conditions, *M. leidyi* spent the majority of the time in the upper portion of the tank (Fig. 4) and occupied a similar mean depth (6.2 ± 2.1 cm in still, 7.4 ± 1.9 in turbulence, Table II). However, *M. leidyi* actively avoided turbulence levels on the order of 10^{-6} W kg^{-1} within the top few centimeters of the turbulence generator (Fig. 4C and D). In addition to avoiding the surface, mean observed speeds and accelerations increased in response to turbulence throughout the tank (Table II). Behavior in turbulence was not uniform with depth; instead, the response to turbulence was most pronounced at the surface of the tank where the turbulence levels were highest (Table III). The observed speed was 2.8 times higher and the acceleration was 4.3 times higher in the top 3 cm of the tank (Table III) when compared with the mean speed and acceleration for the full 30 cm depth of the tank (Table II). Observed speeds in the top several centimeters were also about three times higher than the fluid velocities (Tables I and III) indicating that avoidance of turbulence was an active behavioral response and not simply the result of passive transport. This behavior was surprisingly sensitive to the gradient in turbulence. Even with relatively small changes in turbulence (levels ranged within about one order of magnitude), the highest observed speeds and accelerations occurred where the turbulence levels were greatest and this effect was observed on the scale of cm (Table III). Avoidance of low to moderate levels of turbulence corroborates field data showing that *M. leidyi* maintain deeper depth distributions during wind-mediated turbulence at the sea surface (Mianzan *et al.*, 2010). Previous studies have shown *M. leidyi* to increase swimming speeds in response to gelatinous predators (*Chrysaora quinquecirrha*: Kreps *et al.*, 1997; *Beroe ovata*: Titelman *et al.*, 2012) but this is the first indication that *M. leidyi* can respond to a fluid mechanical signal.

Swimming behavior in turbulence can be considered in the context of the motility number (Mn) which measures the extent to which swimming behavior exceeds background turbulence (Gallager *et al.*, 2004). In the current study, the Mn for *M. leidyi* throughout the tank was ~2 and the Mn for *M. leidyi* in the top 3 cm was ~6. A value for Mn > 1 suggests that behavior exceeds passive transport due to turbulence and Mn > 3 suggests that organisms can aggregate. Though experiments in tanks cannot fully be extrapolated to the field, these Mn

Downloaded from http://plankt.oxfordjournals.org/ at Acquisitions Dept-Serials on September 9, 2014

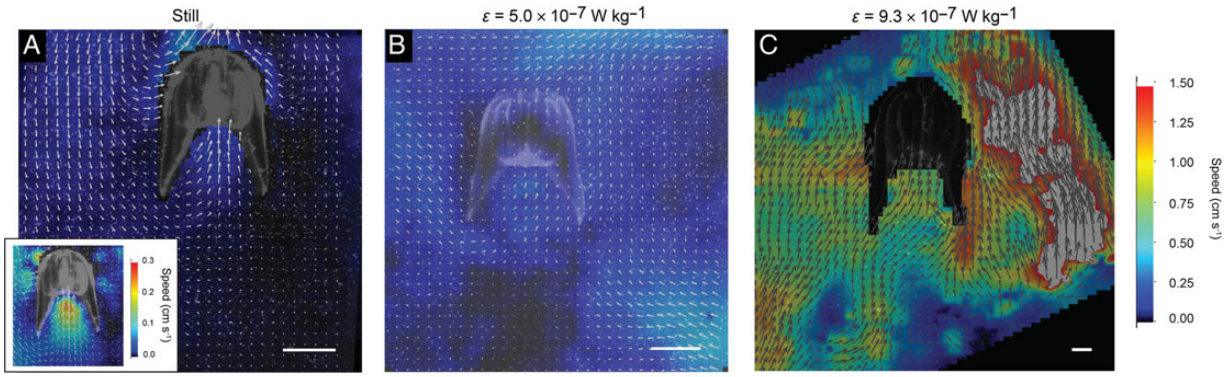

Fig. 7. Instantaneous velocity vectors and speed contours produced by feeding current and background flow in still water (tank) (**A**), $\varepsilon = 5.0 \times 10^{-7}$ W kg^{-1} (tank) (**B**) and $\varepsilon = 9.3 \times 10^{-7}$ W kg^{-1} (field) (**C**). The inset on the left is plotted over a smaller-scale range to more clearly show the signature of the feeding current in still water. Scale bars are 1 cm.

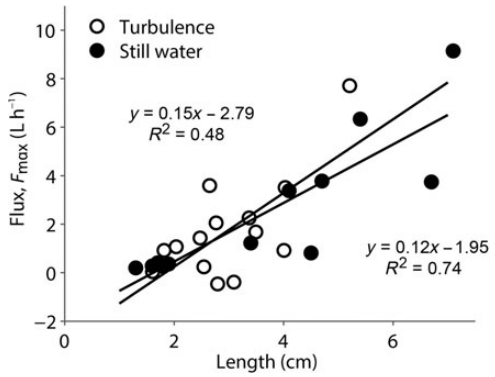

Fig. 8. Fluid flux to *M. leidyi* feeding structures (F_{max}) in still water and in turbulence ($\varepsilon = 2–20 \times 10^{-7}$ W kg^{-1}). F_{max} is a function of the relative velocities of the ctenophore and the fluid and represents a maximum clearance rate. There was no difference in flux in turbulent versus non-turbulent conditions (ANCOVA, $F_{1,22} = 0.38$, $P = 0.54$).

values suggest that *M. leidyi* are capable of aggregating in response to even relatively low levels of turbulence due to avoidance behavior. Again, field observations off the coast of southern Argentina (Costello and Mianzan, 2003) support the notion of behaviorally mediated aggregations in response to turbulence (Mianzan *et al.*, 2010).

Field measurements of turbulence collected during a range of wind speeds in the same shallow region where experimental specimens were collected indicated that wind-driven turbulence declines rapidly with depth (Fig. 3). When wind speeds were relatively low, turbulence approached 10^{-5} W kg^{-1} at the surface but declined to a level below 10^{-6} W kg^{-1} within 2 m of the surface. When wind speeds were higher, turbulence was higher at the surface and also dissipated with depth, approaching 10^{-6} W kg^{-1} near the bottom. In other words, even under windy conditions, there was a refuge at depth from turbulence and our behavior experiments in the laboratory show that *M. leidyi* are capable of seeking out these less turbulent depths. Based on wind speed measurements taken over an entire year, there would almost always be a refuge at depth from wind-driven turbulence at this study site: when ADV measurements were taken during a more windy period, the mean wind speed was 4 m s^{-1} and during 2012, wind speeds exceeded 4.7 m s^{-1} only 5% of the time (Fig. 3D). Though our measurements indicate that turbulent flow is primarily driven by wind at our study site, turbulence is also generated by tides and internal waves. *Mnemiopsis leidyi* could be capable of avoiding higher levels of turbulence throughout the water column, suggesting that turbulence is an important factor in structuring vertical distribution. Additionally, our results suggest that the behavior of *M. leidyi* may result in relatively fine-scale vertical distributions of the ctenophore.

Turbulence avoidance behavior may be important for distribution and ingestion rates of planktonic organisms at the community scale. The few studies examining zooplankton distributions in the field at relevant scales suggest that surface turbulence acts as a cue for downward shifts in vertical distribution (Incze *et al.*, 2001; Maar *et al.*, 2006). By avoiding surface turbulence, *M. leidyi* would spend more time at depth where plankton concentrations might be lower. However, their planktonic prey may simultaneously respond to the same physical cues, although they might be expected to have different thresholds depending on species-specific length scales of sensory structures as well as sensitivity to hydrodynamic cues. In the turbulence generator, the Kolmogorov scale (η) was ~1–2 mm, which is larger than for many planktonic prey. However, the flow below this scale would likely be characterized by shear deformation and zooplankton, including copepods (Fields and Yen, 1997; Kiørboe *et al.*, 1999), and protists (Jakobsen, 2001), are known to detect and respond behaviorally to shear deformation. An understanding of the effect of turbulent

Downloaded from http://plankt.oxfordjournals.org/ at Acquisitions Dept-Serials on September 9, 2014

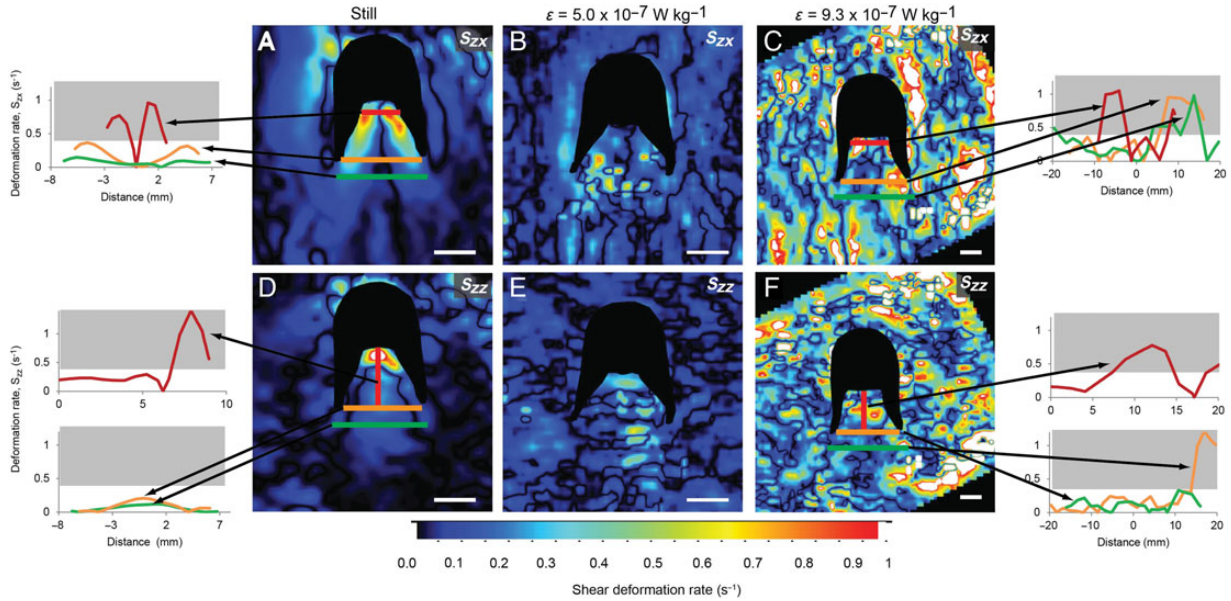

Fig. 9. Instantaneous 2D shear deformation rate contours of the maximum components (S_{zx} and S_{zz}) produced by the *M. leidyi* feeding current and background flow in still water in the tank (**A** and **D**), in turbulence in the tank (**B** and **E**) and in the field (**C** and **F**). Colored transects show shear deformation through feeding regions and outside feeding regions in still water and in turbulence. Grey shaded areas indicate the range of deformation rates that elicit escape responses by common, coastal copepod species, *Acartia* (0.5 s^{-1}), *Centropages* (1.2 s^{-1}), *Tortanus* (0.34 s^{-1}) and *Eurytemora* (0.6 s^{-1}) (Kiørboe *et al.*, 1999; Green *et al.*, 2003; Burdick *et al.*, 2007). Scale bars are 1 cm.

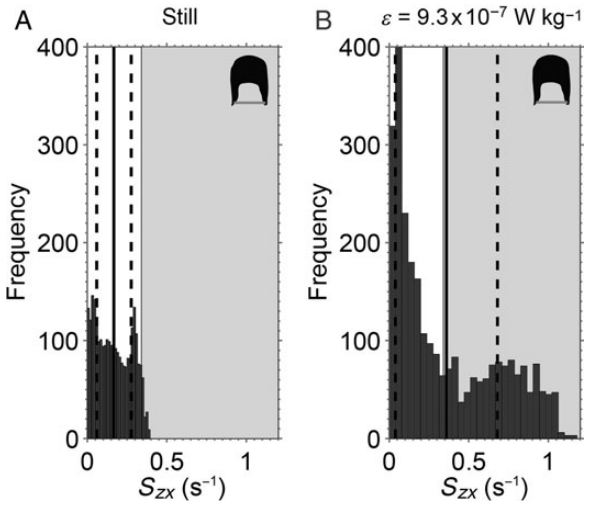

Fig. 10. Frequency histograms showing instantaneous shear deformation rates, S_{zx} (s^{-1}), measured across a transect between the lobe tips over 10 contiguous frames in still water (1.67 s) (**A**) and turbulence (0.33 s) (**B**). Solid black vertical lines show mean shear deformation rate and dashed lines show the standard deviation. Grey shaded areas indicate the range of deformation rates that elicit escape responses from copepod species (as in Fig. 9).

flow on plankton distributions at the community-wide level awaits further field studies but it is likely that encounter and ingestion rates are strongly mediated by vertical patterns of turbulence (Franks, 2001).

Influence of turbulence on feeding currents

In addition to influencing swimming behavior and distribution, laboratory and field turbulence influenced organism-level aspects of *M. leidyi* suspension feeding. Lobe width has been observed to decrease when organisms are disturbed in the field (J. H. Costello, unpublished results). After an initial "startle response", mean lobe width did not change under laboratory turbulence levels, though it was more variable (Fig. 6). The characteristic fluid structure of the feeding current (Colin *et al.*, 2010) was degraded even in moderately low turbulence (Fig. 7). Although models predict potential feeding current erosion in turbulent flows (Kiørboe and Saiz, 1995), there are few direct observations of this in the laboratory (Marrasé *et al.*, 1990) and none, to the best of our knowledge, from the field. In still water, *M. leidyi* produces an organized, laminar feeding current with flow oriented parallel to the lobes and this organized structure extends beyond the lobes (Fig. 7A, Colin *et al.*, 2010). The feeding current is effective of drawing a range of non-motile (e.g. invertebrate larvae, fish eggs), and motile (e.g. copepods, fish larvae) prey types toward the feeding structures (Costello *et al.*, 2012). However, in turbulent flows, feeding currents were eroded beyond the tips of the lobes and even between the lobes, i.e. the flow was much less organized and velocity vectors did not necessarily orient toward the mouth, particularly in the case measured

Downloaded from http://plankt.oxfordjournals.org/ at Acquisitions Dept-Serials on September 9, 2014

from the field (Fig. 7C). Degradation of the feeding current is expected to decrease encounters with prey (Marrasé *et al.*, 1990).

In spite of the decline in the structure of the feeding current, the measured flux to the feeding structures was similar in still water and in turbulence. The flux can be augmented by increasing the speed of the feeding current, increasing swimming speed or increasing the area between the lobes. Lobe width was similar in still water and turbulence (Fig. 6), but *M. leidyi* swam at higher speeds in turbulence (Table I, Fig. 5), suggesting that declining fluid flux within the degraded feeding current was counteracted by increased flows due to higher swimming velocities. More generally, contacts between predator and prey depend on the speed of the predator and the prey. Pelagic suspension feeders can control the relative speed of the prey through an increase in feeding current speed, because prey are drawn in with the fluid, or by increasing their own swimming speed. *Mnemiopsis leidyi* appears to compensate for the decline in fluid delivery to the feeding structures by increasing swimming speed (Table II) and increasing the time spent swimming (Fig. 5). However, this may come at a cost because it has been shown that moving forward while suspension feeding is less efficient than hovering (Lighthill, 1976; Kiørboe, 2011).

The flux of fluid to the feeding structures serves as a proxy for feeding rate but assumes that all prey entrained in the fluid are captured. Flux therefore represents an upper limit to clearance rate whereas in reality, individual predator–prey interactions are more nuanced. Motile zooplankton can respond to shear deformation produced by a predator (by escaping) or by prey (by attacking). However, the presence of background turbulence has been shown to damp the response of copepod prey to predator-like signals, increasing mortality rates (Robinson *et al.*, 2007). In our study, instantaneous shear deformation rates produced by low levels of turbulence exceeded the rates produced by the feeding current, even between the lobes (Figs 9 and 10). Furthermore, the turbulence-induced deformation rates exceeded the threshold required to elicit escape responses from typical copepod prey (Figs 9 and 10). In fact, in the case we examined, 42% of the shear deformation rates (S_{zx}) produced between the lobe tips in background turbulence would be expected to trigger an escape by some copepod species (Fig. 10). In contrast, and consistent with previous data showing that *M. leidyi* is hydrodynamically silent (Colin *et al.*, 2010), only 5% of the deformation rates exceeded this threshold in still water. Previous experiments in still water show that the majority of adult *Acartia tonsa* captured by *M. leidyi* initially contact the oral lobes and not the tentillae or the oral region, which are aboral to the lobes (Fig. 1). Yet, *A. tonsa* contacting the lobes are retained with only ~62% efficiency whereas *A. tonsa* contacting the tentillae are retained with ~85% efficiency (Waggett and Costello, 1999). Therefore, the presence of heightened turbulence at the primary capture surface for copepods (i.e. the oral lobes) would be expected to reduce retention. In other words, the presence of stochastic flow in the background can be expected to diminish the capability of motile prey to detect the presence of *M. leidyi*. Furthermore, *M. leidyi* can also anticipate the presence of a copepod before it contacts the lobes and responds positioning the lobes to minimize escape routes (Costello *et al.*, 1999); the presence of background fluid motion would also be expected to damp this anticipatory response.

Further characterization of realistic levels of turbulence on *M. leidyi* predation, on both motile and non-motile prey, will require direct observations of encounter and capture in addition to ingestion rate measurements. However, the results presented here show that turbulent flows, which are characteristic of the coastal environment, are expected to influence both the vertical distribution and feeding success of *M. leidyi*. Since *M. leidyi* is primarily distributed in shallow, coastal areas in both native and non-native habitats, turbulence is an important environmental parameter that helps determine its trophic role. More broadly, the direct observation that feeding currents are eroded in turbulence suggests that this may be an important factor for other planktonic suspension feeders.

ACKNOWLEDGEMENTS

Comments from two anonymous reviewers strengthened the manuscript. We thank Cornelia Jaspers for help with ADV sampling and Jeremy de Jong for providing Matlab code for calculating dissipation rates.

FUNDING

This research was supported by the National Science Foundation (OCE-1061353 to J.H.C., S.P.C., J.O.D.; OCE-1155084 to K.R.S.) and the Office of Naval Research (N000141010137 to J.O.D., N000140810654 to J.H.C.).

REFERENCES

Acuña, J. L. (2001) Pelagic tunicates: why gelatinous? *Am. Nat.*, **158**, 100–107. doi:10.1086/320864.

Burdick, D. S., Hartline, D. K. and Lenz, P. H. (2007) Escape strategies in co-occurring calanoids copepods. *Limnol. Oceanogr.*, **52**, 2373–2385. doi:10.4319/lo.2007.52.6.2373.

Downloaded from http://plankt.oxfordjournals.org/ at Acquisitions Dept-Serials on September 9, 2014

Colin, S. P., Costello, J. H., Hansson, L. J., Titelman, J. and Dabiri, J. O. (2010) Stealth predation and the predatory success of the invasive ctenophore Mnemiopsis leidyi. *Proc. Natl Acad. Sci. USA*, **107**, 17223–17227. doi:10.1073/pnas.1003170107.

Costello, J. H., Bayha, K. M., Mianzan, H. W. *et al.* (2012) Transitions of *Mnemiopsis leidyi* (Ctenophora: Lobata) from a native to an exotic species: a review. *Hydrobiologia*, **690**, 21–46. doi:10.1007/s10750-012-1037-9.

Costello, J. H., Loftus, R. and Waggett, R. (1999) Influence of prey detection on capture success for the ctenophore *Mnemiopsis leidyi* feeding upon adult *Acartia tonsa* and *Oithona colcarva* copepods. *Mar. Ecol. Prog. Ser.*, **191**, 207–216. doi:10.3354/meps191207.

Costello, J. H. and Mianzan, H. W. (2003) Sampling field distributions of *Mnemiopsis leidyi* (Ctenophora, Lobata): planktonic or benthic methods? *J. Plankton Res.*, **25**, 455–459.

De Jong, J., Cao, L., Woodward, S. H. *et al.* (2009) Dissipation rate estimation from PIV in zero-mean isotropic turbulence. *Exp. Fluids*, **46**, 499–515. doi:10.1007/s00348-008-0576-3.

Dicke, M. and Burrough, P. A. (1988) Using fractal dimensions for characterizing tortuosity of animal trails. *Physiol. Entomol.*, **13**, 393–398. doi:10.1111/j.1365-3032.1988.tb01122.x.

Fields, D. M. and Yen, J. (1997) The escape behavior of marine copepods in response to a quantifiable fluid mechanical disturbance. *J. Plankton Res.*, **19**, 1289–1304. doi:10.1093/plankt/19.9.1289.

Finenko, G. A., Kideys, A. E., Anninsky, B. E. *et al.* (2006) Invasive ctenophore *Mnemiopsis leidyi* in the Caspian Sea: feeding, respiration, reproduction and predatory impact on the zooplankton community. *Mar. Ecol. Prog. Ser.*, **314**, 171–185. doi:10.3354/meps314171.

Franks, P. J. S. (2001) Turbulence avoidance: an alternative explanation of turbulence-enhanced ingestion rates in the field. *Limnol. Oceanogr.*, **46**, 959–963.

Gallager, S. M., Yamazaki, H. and Davis, C. S. (2004) Contribution of fine-scale vertical structure and swimming behavior to formation of plankton layers on Georges Bank. *Mar. Ecol. Prog. Ser.*, **267**, 27–43. doi:10.3354/meps267027.

Green, S., Visser, A. W., Titelman, J. and Kiorboe, T. (2003) Escape responses of copepod nauplii in the flow field of the blue mussel. *Mytilus edulis. Mar. Biol.*, **142**, 727–733.

Incze, L. S., Hebert, D., Wolff, N. *et al.* (2001) Changes in copepod distributions associated with increased turbulence from wind stress. *Mar. Ecol. Prog. Ser.*, **213**, 229–240. doi:10.3354/meps213229.

Jakobsen, H. H. (2001) Escape response of planktonic protists to fluid mechanical signals. *Mar. Ecol. Prog. Ser.*, **214**, 67–78.

Jumars, P. A., Trowbridge, J. H., Boss, E. *et al.* (2009) Turbulence-plankton interactions: a new cartoon. *Mar. Ecol.*, **30**, 133–150. doi:10.1111/j.1439-0485.2009.00288.x.

Katija, K. and Dabiri, J. O. (2008) In situ field measurements of aquatic animal-fluid interactions using a Self-Contained Underwater Velocimetry Apparatus (SCUVA). *Limnol. Oceanogr.-Meth.*, **6**, 162–171. doi:10.4319/lom.2008.6.162.

Kideys, A. E., Roohi, A., Eker-Develi, E. *et al.* (2008) Increased chlorophyll levels in the Southern Caspian Sea following an invasion of jellyfish. *Res. Lett. Ecol.* doi:10.1155/2008/185642.

Kiørboe, T. (2011) How zooplankton feed: mechanisms, traits and trade-offs. *Biol. Rev.*, **86**, 311–339. doi:10.1111/j.1469-185X.2010.00148.x.

Kiørboe, T. and Saiz, E. (1995) Planktivorous feeding in calm and turbulent environments, with emphasis on copepods. *Mar. Ecol. Prog. Ser.*, **122**, 135–145. doi:10.3354/meps122135.

Kiørboe, T., Saiz, E. and Visser, A. (1999) Hydrodynamic signal perception in the copepod *Acartia tonsa*. *Mar. Ecol. Prog. Ser.*, **179**, 97–111. doi:10.3354/meps179097.

Kreps, T. A., Purcell, J. E. and Heidelberg, K. B. (1997) Escape of the ctenophore, *Mnemiopsis leidyi* from the scyphomedusa predator, *Chrysaora quinquecirrha*. *Mar. Biol.*, **128**, 441–446. doi:10.1007/s002270050110.

Lighthill, J. (1976) Flagellar hydrodynamics: the John von Neumann lecture, 1975. *SIAM Rev.*, **18**, 161–230.

Luznik, L., Gurka, R., Nimmo Smith, W. A. M. *et al.* (2007) Distribution of energy spectra, Reynolds stresses, turbulence production, and dissipation in a tidally driven bottom boundary layer. *J. Phys. Oceanogr.*, **37**, 1527–1550. doi:10.1175/JPO3076.1.

Maar, M., Visser, A. W., Nielsen, T. G. *et al.* (2006) Turbulence and feeding behavior affect the vertical distributions of *Oithona similis* and *Microsetella norvegica*. *Mar. Ecol. Prog. Ser.*, **313**, 157–172. doi:10.3354/meps313157.

Marrasé, C., Costello, J. H., Granata, T. *et al.* (1990) Grazing in a turbulent environment: energy dissipation, encounter rates, and efficacy of feeding currents in *Centropages hamatus*. *Proc. Natl Acad. Sci. USA*, **87**, 1653–1657.

Mianzan, H. W., Martos, P., Costello, J. H. *et al.* (2010) Avoidance of hydrodynamically mixed environments by *Mnemiopsis leidyi* (Ctenophora: Lobata) in open-sea populations from Patagonia, Argentina. *Hydrobiologia*, **645**, 113–124. doi:10.1007/s10750-010-0218-7.

Miller, R. J. (1974) Distribution and biomass of an estuarine ctenophore population, *Mnemiopsis leidyi* (A. Agassiz). *Chesapeake Sci.*, **15**, 1–8.

Mills, C. E. (1995) Medusae, siphonophores, and ctenophores as planktivorous predators in changing global ecosystems. *ICES J. Mar. Sci.*, **52**, 575–581. doi:10.1016/1054-3139(95)80072-7.

Mutlu, E. (1999) Distribution and abundance of ctenophores and their zooplankton food in the Black Sea. II. *Mnemiopsis leidyi*. *Mar. Biol.*, **135**, 603–614. doi:10.1007/s002270050661.

Pésceli, H. L., Trulsen, J. and Fiksen, Ø. (2012) Predator–prey encounter and capture rates for plankton in turbulent environments. *Prog. Oceanogr.*, **101**, 14–32.

Peters, F. and Gross, T. (1994) Increased grazing rates of microplankton in response to small-scale turbulence. *Mar. Ecol. Prog. Ser.*, **115**, 299–307.

Peters, F. and Redondo, J. M. (1997) Turbulence generation and measurement: application to studies on plankton. *Sci. Mar.*, **61**, 205–228.

Pitt, K. A., Duarte, C. M., Lucas, C. H. *et al.* (2013) Jellyfish body plans provide allometric advantages beyond low carbon content. *PLoS One*, **8**, e72683. doi:10.1371/journal.pone.0072683.

Prairie, J. C., Sutherland, K. R., Nichols, K. J. *et al.* (2012) Biophysical interactions in the plankton: a cross-scale review. *Limnol. Oceanogr.: Fluids Environ.*, **2**, 121–145. doi:10.1215/21573689-1964713.

Purcell, J. E., Shiganova, T. A., Decker, M. B. *et al.* (2001) The ctenophore Mnemiopsis in native and exotic habitats: U.S. estuaries versus the Black Sea basin. *Hydrobiologia*, **451**, 145–176.

Robinson, H. E., Finelli, C. M. and Buskey, E. J. (2007) The turbulent life of copepods: effects of water flow over a coral reef on their ability to detect and evade predators. *Mar. Ecol. Prog. Ser.*, **349**, 171–181. doi:10.3354/meps07123.

Roohi, A., Kideys, A. E., Sajjadi, A. *et al.* (2009) Changes in biodiversity of phytoplankton, zooplankton, fishes and macrobenthos in the

Downloaded from http://plankt.oxfordjournals.org/ at Acquisitions Dept-Serials on September 9, 2014

southern Caspian Sea after the invasion of the ctenophore *Mnemiopsis leidyi*. *Biol. Invasions.*, **12**, 2343–2361. doi:10.1007/s10530-009-9648-4.

Rothschild, B. J. and Osborn, T. R. (1988) Small-scale turbulence and plankton contact rates. *J. Plankton Res.*, **10**, 465–474. doi:10.1093/plankt/10.3.465.

Saiz, E. and Kiørboe, T. (1995) Predatory and suspension feeding of the copepod *Acartia tonsa* in turbulent environments. *Mar. Ecol. Prog. Ser.*, **122**, 147–158. doi:10.3354/meps122147.

Tanaka, T. and Eaton, J. K. (2007) A correction method for measuring turbulence kinetic energy dissipation rate by PIV. *Exp. Fluids*, **42**, 893–902. doi:10.1007/s00348-007-0298-y.

Titelman, J., Hansson, L. J., Nilsen, T. *et al.* (2012) Predator-induced vertical behavior of a ctenophore. *Hydrobiologia*, **690**, 181–187. doi:10.1007/s10750-012-1056-6.

Waggett, R. and Costello, J. H. (1999) Different mechanisms used by the lobate ctenophore, *Mnemiopsis leidyi*, to capture nauplii and adult life stages of the copepod *Acartia tonsa*. *J. Plankton Res.*, **21**, 2037–2052. doi:10.1093/plankt/21.11.2037.

Warnaars, T. A., Hondzo, M. and Carper, M. A. (2006) A desktop apparatus for studying interactions between microorganisms and small-scale fluid motion. *Hydrobiologia*, **563**, 431–443. doi:10.1007/s10750-006-0030-6.

Downloaded from http://plankt.oxfordjournals.org/ at Acquisitions Dept-Serials on September 9, 2014